J. Fluid Mech. (1995), *vol.* 297, *pp.* 307–325

Edge waves along periodic coastlines. Part 2

By D. V. EVANS AND M. FERNYHOUGH
School of Mathematics, University of Bristol, Bristol BS8 1TW, UK

(Received 16 January 1995 and in revised form 15 March 1995)

Numerical evidence of the existence of edge waves travelling along a periodic coastline consisting of a straight and vertical cliff face from which protrudes an infinite number of identical rectangular barriers, each extending throughout the water depth, is given based on a Galerkin approximation to an integral representation of the problem derived using the linear theory of water waves.

1. Introduction

In a recent paper, Evans & Linton (1993, refered to herein as Part 1) using classical linear water wave theory, proved the existence of edge waves travelling along a periodic coastline consisting of a straight and vertical cliff face from which protruded an infinite number of identical thin barriers, each extending throughout the water depth, provided the barriers were sufficiently long. Because the depth dependence could be separated out, the problem reduced to the solution of the two-dimensional Helmholtz equation, and was identical to an appropriate problem in linear acoustics, optics or electromagnetism involving a 'comb-like' diffraction grating.

A general discussion of the electromagnetic theory of gratings is given by Petit (1980) and a more mathematical treatment by Wilcox (1984). In particular it is shown that there are two types of expressions which occur in a Fourier-series representation of the field, one describing plane waves which are either incident upon or scattered by the grating, the other describing Rayleigh–Bloch surface waves which are confined to the vicinity of the grating, and which decay exponentially in a direction normal to the grating. The question as to whether Rayleigh–Bloch surface waves can exist in isolation in the absence of incident or reflected plane waves is mentioned in Wilcox (1984, pp. 11–12) who states that no general criteria are known on the shape of the grating for these surface waves to exist. However if the Neumann condition on the grating is replaced by a Dirichlet condition it would appear that no surface waves can exist in isolation.

In Part 1 a rigorous proof of the existence of Rayleigh-Bloch surface waves was given for the case of a 'comb-like' grating provided the 'teeth' of the comb were sufficiently long. The solution was in the form of the usual Fourier expansion appropriate to the periodicity of the grating modulated by a factor $\exp(\mathrm{i}\beta y)$ where y is measured along the grating. The form of the solution provided an accurate and efficient method for obtaining, for a given k and hence frequency $\omega/2\pi$, the corresponding value(s) of β for surface waves to exist. In the acoustic case, we have $k = \omega/c_v$ where c_v is the velocity of sound, whilst in the water wave case, k is the real positive root of $\omega^2 = gk\tanh kh$ where h is the uniform depth of water, and the solutions are more commonly referred to as edge waves.

Such edge waves are common in classical linear water wave theory but only when

the bottom topography is non-uniform. The simplest such solution is that found by Stokes (1846) for a uniformly sloping beach. The solution, in the form of a single exponential term, was generalized by Ursell (1952) who showed that more and more edge wave modes are possible as the beach slope tends to zero. It is known that edge waves exist whenever a shallow region is joined to a deeper region offshore and Jones (1953) proved that at least one such mode exists in this situation.

If the depth of the fluid is constant everywhere it is not obvious that edge waves can exist. For example the only solution in a region of constant depth bounded by a vertical impervious cliff, for waves propagating in the direction of the cliff, is a simple plane wave which does not decay in the direction normal to the cliff, and is not an edge wave. However, as shown in Part 1, if there exists an infinite set of equally spaced identical thin vertical impervious barriers extending outwards in a direction normal to the cliff and throughout the water depth, edge waves do exist.

A special case of these progressing edge waves described in Part 1 is that of standing edge waves and, by symmetry, the problem reduces in this case to a thin barrier protruding from a vertical wall and mid-way between two parallel vertical walls extending out to infinity. Neumann conditions are to be satisfied on the barrier and the walls and a Dirichlet condition, corresponding to antisymmetric standing waves, is to be satisfied on the extension of the barrier out to infinity. This latter condition ensures that a cut-off frequency exists and enables standing edge waves or trapped modes to be constructed as described in Evans (1992). Previously Evans & Linton (1991) have used the method of matched eigenfunction expansions to show numerically that such trapped modes occurred when the barrier was replaced by a rectangular block, symmetric about the centreline.

In the present paper we take advantage of an idea due to Porter (1995) to improve upon this method and obtain accurate estimates of the relation between frequency and dominant long-shore wavenumber for the generalized problem of progressing edge waves along a periodic array of rectangular blocks, the results of Evans & Linton (1991) being recovered as a special case.

The problem is formulated in § 2 where it is shown how the existence of progressing edge waves reduces to the problem of whether a certain equation ((2.31) below) has a solution where the unknown $u(y)$ satisfies (2.27). Rather than attempt to solve (2.27) exactly a Galerkin approximation is used in which the expansion functions for $u(y)$ are chosen to model the known singularities at the end points of the integral corresponding to the corners of the blocks, and also chosen to provide maximum simplification of the results.

The method turns out to be extremely efficient with no more than five expansion functions necessary to give three-figure accuracy.

The results are described in § 3 where it is shown that for any choice of geometry of the blocks, and choice of fundamental wavenumber βd, there exists a value of kd and hence wave frequency from which the overall progressing edge wave can be constructed. The resulting free-surface elevations are illustrated in a variety of cases, showing how in general, except for special values of βd, the motion is aperiodic in a direction parallel to the cliff face, whilst decaying to zero out to sea.

2. Formulation and solution

Cartesian coordinates are chosen and the dimensions of the blocks are illustrated in figure 1. Because they extend throughout the water depth we can write the harmonic

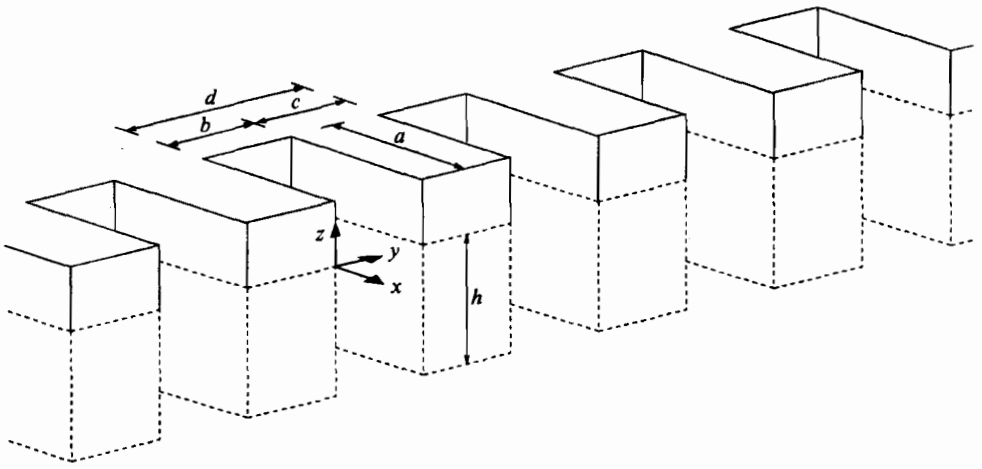

FIGURE 1. Coastline consisting of a periodic rectangular array.

velocity potential Φ in the from

$$\Phi(x, y, z, t) = \mathrm{Re}\left\{\phi(x, y) \cosh k(z + h)\, \mathrm{e}^{-\mathrm{i}\omega t}\right\}, \tag{2.1}$$

where h is the water depth, ω the assumed radian frequency of the edge waves and k is the real positive root of

$$\omega^2 = gk \tanh kh. \tag{2.2}$$

In the context of acoustics (2.2) is replaced by

$$\omega^2 = kc_v, \tag{2.3}$$

where c_v is the velocity of sound. On the basis of either linear acoustics or water waves, we seek a non-trivial $\phi(x, y)$ satisfying

$$\left(\nabla^2 + k^2\right) \phi = 0 \tag{2.4}$$

in the fluid,

$$\frac{\partial \phi}{\partial n} = 0 \tag{2.5}$$

on all rigid boundaries, and

$$\phi \to 0, \quad x \to \infty, \quad \text{for all } y. \tag{2.6}$$

One argument for believing that solutions to these equations exist is as follows. Imagine that the inner fluid region $x < 0$ extends to $x = -\infty$ and consider a simple plane wave $\exp(\mathrm{i}kx)$ progressing from $x = -\infty$ in $0 < y < b$ and, in general, a plane wave $\exp(\mathrm{i}kx + \mathrm{i}md\beta)$ from $x = -\infty$ in $md < y < md + b$, for all integers m, where β is at our disposal. These waves will be partially reflected and partially transmitted into $x > 0$ when reaching $x = 0$, but the assumed form of the incident waves together with the periodic geometry requires that the solution everywhere in the fluid region must satisfy

$$\phi(x, y + md) = \mathrm{e}^{\mathrm{i}md\beta} \phi(x, y), \quad m = 0, \pm 1, \pm 2, \ldots \tag{2.7}$$

since the only difference observed in moving through a period d in the y-direction is in the change of phase of the assumed form of the incident waves in $x < 0$.

Equation (2.7) is satisfied by

$$\phi(x, y) = e^{i\beta y}\psi(x, y), \tag{2.8}$$

where $\psi(x, y)$ is periodic with period d.

It follows from (2.4) by separation of variables that we may write, in $x \geqslant 0$

$$\phi(x, y) = \sum_{n=-\infty}^{\infty} A_n e^{-\gamma_n x}\Psi_n(y), \tag{2.9}$$

where

$$\Psi_n(y) = e^{i\beta_n y}, \quad \beta_n = \beta + \frac{2n\pi}{d} \tag{2.10}$$

satisfies

$$\frac{1}{d}\int_0^d \Psi_m(y)\overline{\Psi_n(y)}\,dy = \delta_{mn} \tag{2.11}$$

and the bar denotes complex conjugate.

Also

$$\gamma_n = (\beta_n^2 - k^2)^{1/2} > 0 \tag{2.12}$$

provided $k < \beta < 2\pi/d - k$ which we shall assume is satisfied.

It follows that for this new problem it is possible to choose $\beta > 0$ such that there is no radiation into $x > 0$ and in each region $md < y < md + b$ there must exist a reflected wave having a reflection coefficient R satisfying $|R| = 1$. It is now possible to use the argument applied in Evans & Linton (1991) to the simpler problem of a rectangular block in a channel. If the extent of the inner fluid region is finite but large, an approximate solution is obtained from the solution to this new problem by ensuring that the total wave field, incident plus reflected waves, has zero normal derivative on the back face of the inner region $x = -a$. This results in

$$R = e^{-2ika} \tag{2.13}$$

as an approximation to the condition for edge waves, where R is the reflection coefficient defined above.

Since this new problem described above cannot be solved explicitly, except in the case $b = 0$, $k > \beta$ (Mittra & Lee 1971, p. 50) we shall make no further use of (2.13) other than to remark that the above discussion gives added plausibility to the existence of progressive edge waves, and also provides us with a starting point for their construction.

Thus it is natural to assume that the form of the solution in $x > 0$ is indeed given by (2.9)–(2.11) with the restriction

$$0 < k < \beta < 2\pi/d - k. \tag{2.14}$$

Thus the edge-wave solution is given by (2.9) once the A_n, β and k are known. It will be shown that a solution can be obtained only for a particular relation between β and k which will be derived. Note that the form of (2.9) is complicated, being an infinite sum of modes each of which describes an edge wave travelling parallel to the cliff face and decaying exponentially out to sea. Thus the nth such mode has amplitude proportional to $|A_n|$, wavelength $\lambda_n = 2\pi/|\beta + 2n\pi/d|$ and travels in a direction dictated by the sign of β_n. The longest of these modes is that corresponding to $n = 0$, having wavelength $2\pi/\beta$, and travels in the positive y-direction.

Now in the region $-a \leqslant x \leqslant 0, 0 \leqslant y \leqslant b$ we write

$$\phi(x,y) = \sum_{n=0}^{\infty} B_n^{(0)} \cosh \alpha_n(x+a)\psi_n(y) \tag{2.15}$$

where

$$\alpha_n = (p_n^2 - k^2)^{1/2}, \quad \alpha_0 = -\mathrm{i}k$$

and where

$$\psi_n(y) = \varepsilon_n^{1/2} \cos p_n y, \quad p_n = n\pi/b,$$

with

$$\varepsilon_0 = 1, \quad \varepsilon_n = 2, \quad n \geqslant 1 \tag{2.16}$$

satisfies

$$\frac{1}{b}\int_0^b \psi_m(y)\psi_n(y)\,\mathrm{d}y = \delta_{mn}. \tag{2.17}$$

Here we assume $k < \pi/b$ so that $\alpha_n > 0$, $n > 0$. This will turn out to be satisfied automatically since we will show that it is only necessary to consider $\beta \leqslant \pi/d$, the condition for an edge-wave solution corresponding to $\beta' = 2\pi/d - \beta$ being the same as for β. It follows that $k < \beta \leqslant \pi/d \leqslant \pi/b$ and only one mode can propagate into $x < 0$.

Returning to (2.7) and defining

$$\phi(x, y + md) = \sum_{n=0}^{\infty} B_n^{(m)} \cosh \alpha_n(x+a)\psi_n(y) \tag{2.18}$$

we see that (2.7) is satisfied provided

$$B_n^{(m)} = \mathrm{e}^{\mathrm{i}m\beta d} B_n^{(0)}. \tag{2.19}$$

Equation (2.18) provides the extension of $\phi(x,y)$ to $-a \leqslant x \leqslant 0$, $md \leqslant y \leqslant md + b$ ensuring that conditions (2.4), (2.5) are satisfied. It is only necessary therefore to consider the interval $0 \leqslant y \leqslant d$ and to require ϕ, ϕ_x continuous on

$$L_g : \{x = 0, 0 \leqslant y \leqslant b\} \tag{2.20}$$

and $\phi_x = 0$ on

$$L_b : \{x = 0, b \leqslant y \leqslant d\}. \tag{2.21}$$

Now from (2.9) and (2.15)

$$\phi_x|_{x=0} \equiv U(y) = \sum_{n=-\infty}^{\infty} (-\gamma_n) A_n \Psi_n(y) = \begin{cases} \displaystyle\sum_{n=0}^{\infty} \alpha_n B_n^{(0)} \sinh \alpha_n a \psi_n(y), & y \in L_g, \\ 0, & y \in L_b. \end{cases} \tag{2.22}$$

We now multiply (2.22) by $\overline{\Psi_m(y)}$ and integrate over $[0,d]$ using (2.11), to obtain

$$(-\gamma_m)A_m = \frac{1}{d}\int_{L_g} U(y)\overline{\Psi_m(y)}\,\mathrm{d}y \tag{2.23}$$

where (2.21) has been used.

Again, multiplying (2.22) by $\psi_m(y)$ and integrating over L_g gives

$$\alpha_m B_m^{(0)} \sinh \alpha_m a = \frac{1}{b}\int_{L_g} U(y)\psi_m(y)\,\mathrm{d}y = \frac{1}{b}U_m, \tag{2.24}$$

say. Continuity of ϕ on L_g requires from (2.9), (2.15)

$$\sum_{n=-\infty}^{\infty} A_n \Psi_n(y) = \sum_{n=0}^{\infty} B_n^{(0)} \cosh \alpha_n a \psi_n(y), \quad y \in L_g \tag{2.25}$$

and substituting for A_n, $B_n^{(0)}$ in (2.25) from (2.23), (2.24), extracting the term involving $B_0^{(0)}$ and defining

$$U(y) = \frac{\cot ka}{kb} U_0 u(y) \tag{2.26}$$

gives

$$\int_{L_g} u(t) K(y,t)\, \mathrm{d}t = \psi_0(y) \tag{2.27}$$

and

$$\int_{L_g} u(y) \psi_0(y)\, \mathrm{d}y = kb \tan ka \tag{2.28}$$

where

$$K(y,t) = \sum_{n=1}^{\infty} \frac{\coth \alpha_n a}{\alpha_n b} \psi_n(y) \psi_n(t) + \sum_{n=-\infty}^{\infty} \frac{1}{\gamma_n d} \Psi_n(y) \overline{\Psi_n(t)}. \tag{2.29}$$

The problem has been reduced to first solving (2.27) for $u(y)$, for a given set of geometric parameters and wavenumber β, and then seeking a relationship between β and, say, ka, or kb for which (2.28) is satisfied.

We shall adopt a Galerkin approach to the equations (2.27), (2.28) which we first write in the operator form

$$\mathscr{K} u = \psi_0 \tag{2.30}$$

with

$$(u, \psi_0) = A \equiv kb \tan ka \tag{2.31}$$

where we define the complex inner product by

$$(u, v) = \overline{(v, u)} = \int_{L_g} u(y) \overline{v(y)}\, \mathrm{d}y. \tag{2.32}$$

Note that ψ_0 is real, and from (2.30), (2.31) $A = (u, \mathscr{K} u)$.

Now from (2.29)

$$\overline{K(y,t)} = K(t,y) \tag{2.33}$$

and it follows that

$$(u, \mathscr{K} v) = (\mathscr{K} u, v). \tag{2.34}$$

Further if $v = u$

$$\begin{aligned}(u, \mathscr{K} u) &= \int_{L_g} u(y) \int_{L_g} \overline{K(y,t) u(t)}\, \mathrm{d}t\, \mathrm{d}y \\ &= \sum_{n=1}^{\infty} \frac{\coth \alpha_n a}{\alpha_n b} \left| \int_{L_g} u(y) \psi_n(y)\, \mathrm{d}y \right|^2 + \sum_{n=-\infty}^{\infty} \frac{1}{\gamma_n d} \left| \int_{L_g} u(y) \overline{\Psi_n(y)}\, \mathrm{d}y \right|^2 \geqslant 0 \end{aligned} \tag{2.35}$$

provided the infinite series converge. Thus $A = (u, \psi_0) = (u, \mathscr{K} u) \geqslant 0$ also.

Up until this point the analysis has been exact. Despite the fact that $K(y,t)$ is complex, we have shown that for u satisfying (2.27), $A = (u, \psi_0)$ is real and non-negative so that the edge waves will exist if we can find solutions of $A = kb \tan ka$.

We now show that the value of A for a given β in $k < \beta < \pi/d$ is identical to that obtained for $\beta' = 2\pi/d - \beta$. That is, in an obvious notation

$$A(\beta) = A(\beta'). \tag{2.36}$$

First we note that

$$\beta_{-n-1} = -\left(\beta' + \frac{2n\pi}{d}\right) = -\beta'_n \tag{2.37}$$

so that

$$\gamma_{-n-1} = \gamma'_n = \left(\beta'^2_n - k^2\right)^{1/2}. \tag{2.38}$$

Now in the second series in (2.29) we can replace n by $-n-1$ without affecting the sum. It follows that

$$K(y,t;\beta') = \overline{K(y,t;\beta)} \tag{2.39}$$

in an obvious notation.

Thus, $A(\beta') = (v, \psi_0)$ where v satisfies

$$\overline{\mathscr{K}} v = \psi_0$$

from (2.39), or

$$\mathscr{K}\bar{v} = \psi_0 \tag{2.40}$$

after taking complex conjugate.

Thus, $A(\beta') = (v,\psi_0) = \overline{(\psi_0, v)} = (\psi_0, \bar{v}) = (\mathscr{K}\bar{v}, \bar{v}) = (\bar{v}, \mathscr{K}\bar{v})$ from (2.34), and finally from (2.40)

$$A(\beta') = A(\beta). \tag{2.41}$$

Thus it is only necessary to consider $k < \beta < \pi/d$.

Rather than solve (2.27) directly, the Galerkin method seeks an approximation $u \approx U$ such that

$$(U, \mathscr{K}U) = (U, \psi_0) \tag{2.42}$$

whence the approximation to A is

$$\tilde{A} = (U, \psi_0). \tag{2.43}$$

Now

$$\begin{aligned} A - \tilde{A} &= (u,\psi_0) - (U,\psi_0) \\ &= (u,\psi_0) - (U,\psi_0) - (\psi_0, U) + (U,\psi_0), \end{aligned}$$

trivially since $\tilde{A} = (U,\psi_0) = (\psi_0, U)$ is real.

So,

$$\begin{aligned} A - \tilde{A} &= (u, \mathscr{K}u) - (U, \mathscr{K}u) - (\mathscr{K}u, U) + (U, \mathscr{K}U) \\ &= (u, \mathscr{K}u) - (U, \mathscr{K}u) - (u, \mathscr{K}U) + (U, \mathscr{K}U) \\ &= (u - U, \mathscr{K}(u - U)) \geqslant 0 \end{aligned}$$

where (2.34) and (2.42) has been used.

Thus,

$$\tilde{A} \leqslant A \tag{2.44}$$

and we have a lower bound on the true value of A.

We choose

$$u(y) \approx U = \sum_{n=0}^{N} a_n u_n(y) \tag{2.45}$$

for some $u_n(y)$ and unknown a_n, substitute into (2.30), multiply by $\overline{u_m(y)}$ and integrate over L_g to obtain

$$\sum_{n=0}^{N} a_n K_{mn} = F_{m0}, \quad m = 0, 1, 2, \ldots \tag{2.46}$$

where

$$K_{mn} = (\mathscr{K} u_n, u_m), \tag{2.47}$$

$$F_{m0} = (\psi_0, u_m). \tag{2.48}$$

Then

$$\tilde{A} = \sum_{n=0}^{N} a_n \overline{F_{n0}} \tag{2.49}$$

and it is easily shown that (2.42), (2.43) are equivalent to (2.46), (2.47), using (2.45).

If (2.29) is used in (2.46) we obtain

$$K_{mn} = \sum_{r=1}^{\infty} \frac{\coth \alpha_r a}{\alpha_r b} F_{mr} \overline{F_{nr}} + \sum_{r=-\infty}^{\infty} \frac{1}{\gamma_r d} G_{mr} \overline{G_{nr}} \tag{2.50}$$

where

$$F_{mn} = (\psi_n, u_m) = \int_0^b \psi_n(y) \overline{u_m(y)} \, \mathrm{d}y, \tag{2.51}$$

$$G_{mn} = (\Psi_n, u_m) = \int_0^b \Psi_n(y) \overline{u_m(y)} \, \mathrm{d}y. \tag{2.52}$$

Basis functions for the Galerkin method

It remains to choose the set of functions $u_n(y)$. This is dictated by the two requirements of correct physical modelling and simplicity of the final forms. Thus since $u(y)$ is proportional to the velocity of the flow in the gap L_g, we might expect that sufficiently close to the edges at $y = 0$, $y = b$, $u(y) \sim Cy^{-1/3}(b - y)^{-1/3}$ corresponding to the flow of an ideal fluid round a corner and derived by a simple conformal mapping argument.

In order to preserve simple forms for F_{mn}, G_{mn} and hence K_{mn}, we choose

$$u_m(y) = \frac{\mathrm{i}^m m! \Gamma(1/6)}{\sqrt{2\pi} \Gamma(m + \frac{1}{3})(yb)^{1/3}(b - y)^{1/3}} C_m^{1/6}\left(\frac{2y - b}{b}\right) \tag{2.53}$$

where

$$C_n^{\nu}(\cos\theta) = \sum_{m=0}^{n} \frac{\Gamma(\nu + m)\Gamma(\nu + n - m)}{m!(n - m)![\Gamma(\nu)]^2} \cos(n - 2m)\theta \tag{2.54}$$

are the ultraspherical Gegenbauer polynomials satisfying $C_n^{\nu}(-x) = (-1)^n C_n^{\nu}(x)$. See for example, Erdélyi *et al.* (1954, pp. 38 and 94), where the results

$$\int_0^1 (1-t^2)^{-1/3} C_{2n}^{1/6}(t) \cos yt \, \mathrm{d}t = (-1)^n P_{2n}(y), \tag{2.55}$$

$$\int_0^1 (1-t^2)^{-1/3} C_{2n+1}^{1/6}(t) \sin yt \, \mathrm{d}t = (-1)^n P_{2n+1}(y) \tag{2.56}$$

where

$$P_n(y) = \frac{\pi \Gamma(n+\frac{1}{3}) J_{n+1/6}(y)}{n! \Gamma(\frac{1}{6})(2y)^{1/6}} \tag{2.57}$$

are given. The idea of using the form (2.53) for $u_m(y)$ was suggested by Porter (1995). See also Porter & Evans (1995). We emphasize that the rather curious form of (2.53) is chosen solely to both model the physical behaviour of the field near the sharp corners and to provide simplification of the final results. See (2.58)–(2.60).

After considerable algebra it can be shown that

$$\overline{F_{m0}} = \frac{6}{2^{1/6}\Gamma(\frac{1}{6})} \delta_{m0}, \tag{2.58}$$

$$\overline{F_{mn}} = \varepsilon_n^{1/2} \, \mathrm{i}^m \cos \frac{\pi}{2}(m+n) \left(\frac{2}{n\pi}\right)^{1/6} J_{m+1/6}\left(\frac{n\pi}{2}\right) \tag{2.59}$$

and

$$\overline{G_{mn}} = \mathrm{e}^{-\mathrm{i}\beta_n b/2} \left(\frac{2}{\beta_n b}\right)^{1/6} J_{m+1/6}\left(\frac{\beta_n b}{2}\right). \tag{2.60}$$

Now returning to (2.23), (2.24) and using (2.26), (2.45), (2.51) and (2.52) we can express A_n and $B_n^{(0)}$ as

$$A_n = -\frac{S}{\gamma_n d} \sum_{m=0}^{N} a_m \overline{G_{mn}} \tag{2.61}$$

and

$$B_n^{(0)} = \frac{S}{\alpha_n b \sinh \alpha_n a} \sum_{m=0}^{N} a_m \overline{F_{mn}} \tag{2.62}$$

where

$$S = \frac{\cot ka}{kb} U_0. \tag{2.63}$$

Thus from (2.50), (2.59) and (2.60)

$$K_{mn} = \sum_{r=1}^{\infty} P_{rmn} \frac{\coth \alpha_r a}{\alpha_r b} \left(\frac{2}{\pi r}\right)^{1/3} J_{m+1/6}\left(\frac{r\pi}{2}\right) J_{n+1/6}\left(\frac{r\pi}{2}\right)$$
$$+ \sum_{r=-\infty}^{\infty} \frac{1}{\gamma_r d} \left(\frac{2}{\beta_r b}\right)^{1/3} J_{m+1/6}\left(\frac{\beta_r b}{2}\right) J_{n+1/6}\left(\frac{\beta_r b}{2}\right) \tag{2.64}$$

where

$$P_{rmn} = \tfrac{1}{2}\{(-1)^r + (-1)^m\}\{(-1)^r + (-1)^n\}. \tag{2.65}$$

Notice that K_{mn} is real and, since the same is true for F_{m0} it follows from (2.46) that the a_m ($m = 0, 1, 2, \ldots$) are real also. This has been achieved by the choice of constant

factors in (2.53). A different choice may have produced a complex K_{mn} but the final form for $\tilde{A}$ from (2.49) would, by virtue of (2.35), still have been real.

The form of the edge wave is now obtained by using (2.61) and (2.9) to give

$$\phi(x,y;\beta) = \sum_{n=-\infty}^{\infty} A'_n \, \mathrm{e}^{\mathrm{i}\beta_n(y-b/2)} \, \mathrm{e}^{-\gamma_n x} \tag{2.66}$$

where

$$A'_n = A_n \, \mathrm{e}^{\mathrm{i}\beta_n b/2} = -\frac{S}{\gamma_n d}\left(\frac{2}{\beta_n b}\right)^{1/6} \sum_{m=0}^{N} a_m J_{m+1/6}\left(\frac{\beta_n b}{2}\right). \tag{2.67}$$

Replacing n by $-n-1$ in (2.66) and using (2.37), (2.38) gives

$$\phi(x,y;\beta) = \sum_{n=-\infty}^{\infty} A'_n(\beta') \, \mathrm{e}^{-\mathrm{i}\beta'_n(y-b/2)} \, \mathrm{e}^{-\gamma'_n x} \tag{2.68}$$

where the result

$$A'_{-n-1}(\beta) = A'_n(\beta') \tag{2.69}$$

has been used.

It follows that

$$\phi(x,y;\beta) = \overline{\phi(x,y;\beta')} \tag{2.70}$$

so that the solution for a value $\beta' = 2\pi/d - k$ differs from the solution for β only in a change of the sign of $(y-b/2)$.

When

$$\beta = \beta' = \pi/d, \tag{2.71}$$

and

$$A'_{-n-1} = A'_n \tag{2.72}$$

then

$$\phi(x,y) = 2\sum_{n=0}^{\infty} A'_n \cos\beta_n\left(y-\frac{b}{2}\right) \, \mathrm{e}^{-\gamma_n x} \tag{2.73}$$

where $\beta_n = (2n+1)\pi/d$, $\gamma_n = (\beta_n^2 - k^2)^{1/2}$.

Clearly from (2.73) ϕ is a standing wave and, since $\phi = 0$, $y = (b-d/2)$ and $\phi_y = 0$, $y = b/2$, $b/2 \pm d$, we have recovered the antisymmetric trapped waves described by Evans & Linton (1991) for a rectangular section of width b placed mid-way between the walls of a channel of width d. Note that a similar limiting case was considered in Part 1 to recover the solution described in Evans (1992) although equation (2.20) of Part 1 contains typographical errors.

Since there is no forcing in the problem we can rescale the surface profiles arbitrarily. For simplicity we choose $S = -1$ so that the scaled surface elevations can be written with time dependence for $x \geqslant 0$ as

$$\eta(x,y,t) = \sum_{n=-\infty}^{\infty} Q_n \, \mathrm{e}^{-\gamma_n x} \cos\left\{\beta_n\left(y-\frac{b}{2}\right) - \omega t\right\} \tag{2.74}$$

where Q_n is real and is given by

$$Q_n = \frac{1}{\gamma_n d}\left(\frac{2}{\beta_n b}\right)^{1/6} \sum_{m=0}^{N} a_m J_{m+1/6}\left(\frac{\beta_n b}{2}\right) \tag{2.75}$$

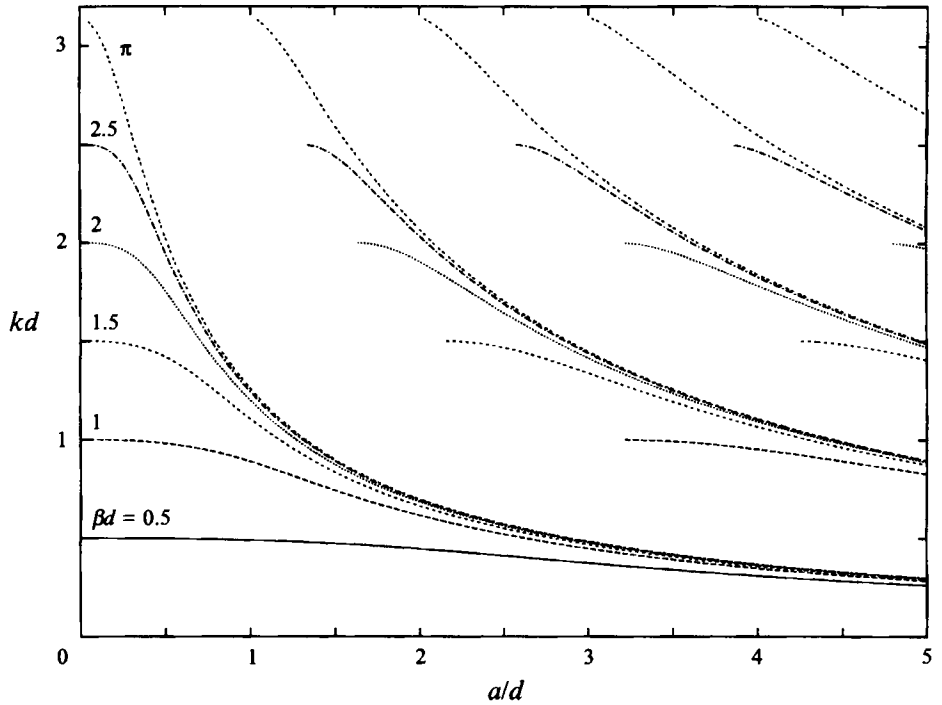

FIGURE 2. Plots of kd against a/d for various values of βd where $b/d = 0.4$. Note that as a/d increases the number of roots increases for a fixed βd.

and for the regions $-a \leqslant x \leqslant 0$, $md \leqslant y \leqslant md + b$ the scaled surface elevation is written for $m = 0, \pm 1, \pm 2, \ldots$ as

$$\eta(x, y + md, t) = \frac{\cos k(x+a)}{\cos ka} \cos(m\beta d - \omega t) - 2\cos(m\beta d - \omega t) \sum_{n=1}^{\infty} R_n \frac{\cosh \alpha_n (x+a)}{\sinh \alpha_n a} \cos\left(\frac{n\pi y}{b}\right) - 2\sin(m\beta d - \omega t) \sum_{n=1}^{\infty} S_n \frac{\cosh \alpha_n (x+a)}{\sinh \alpha_n a} \cos\left(\frac{n\pi y}{b}\right) \tag{2.76}$$

where R_n and S_n are real and given by

$$R_n = \frac{1}{\alpha_n b}\left(\frac{2}{n\pi}\right)^{1/6} \cos\left(\frac{n\pi}{2}\right) \sum_{m=0, m \text{ even}}^{N} a_m J_{m+1/6}\left(\frac{n\pi}{2}\right) \tag{2.77}$$

and

$$S_n = \frac{1}{\alpha_n b}\left(\frac{2}{n\pi}\right)^{1/6} \sin\left(\frac{n\pi}{2}\right) \sum_{m=1, m \text{ odd}}^{N} a_m J_{m+1/6}\left(\frac{n\pi}{2}\right). \tag{2.78}$$

3. Results

In order to determine the relationship between β and k for edge waves to exist we need first to solve (2.46) for the a_m, and then compute $\tilde{A}$ from (2.49). Finally using

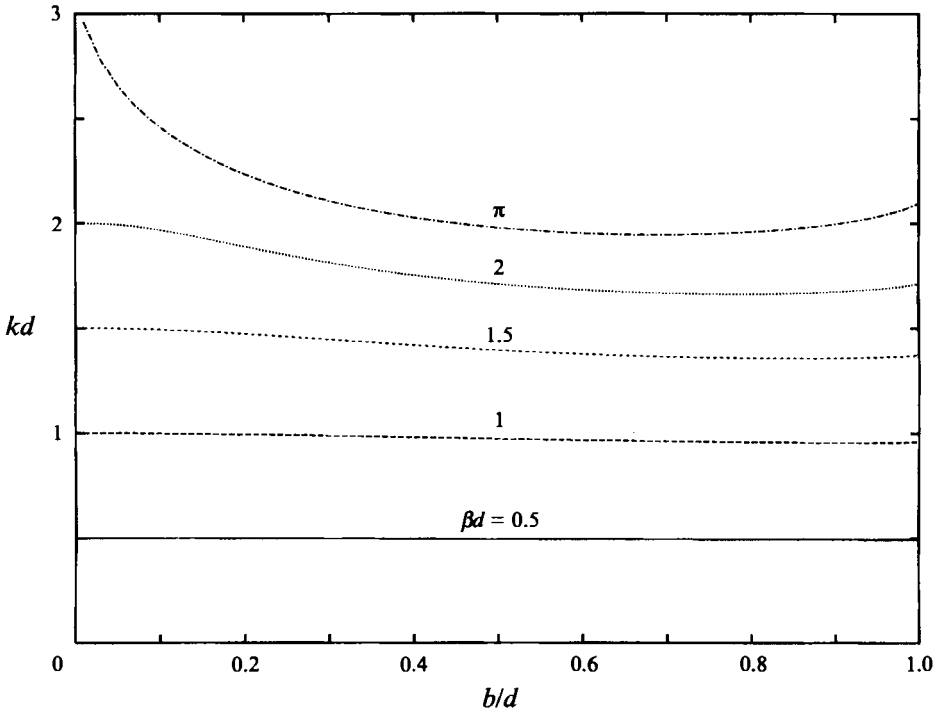

FIGURE 3. Plots of kd against b/d for various values of βd where $a/d = 0.5$.

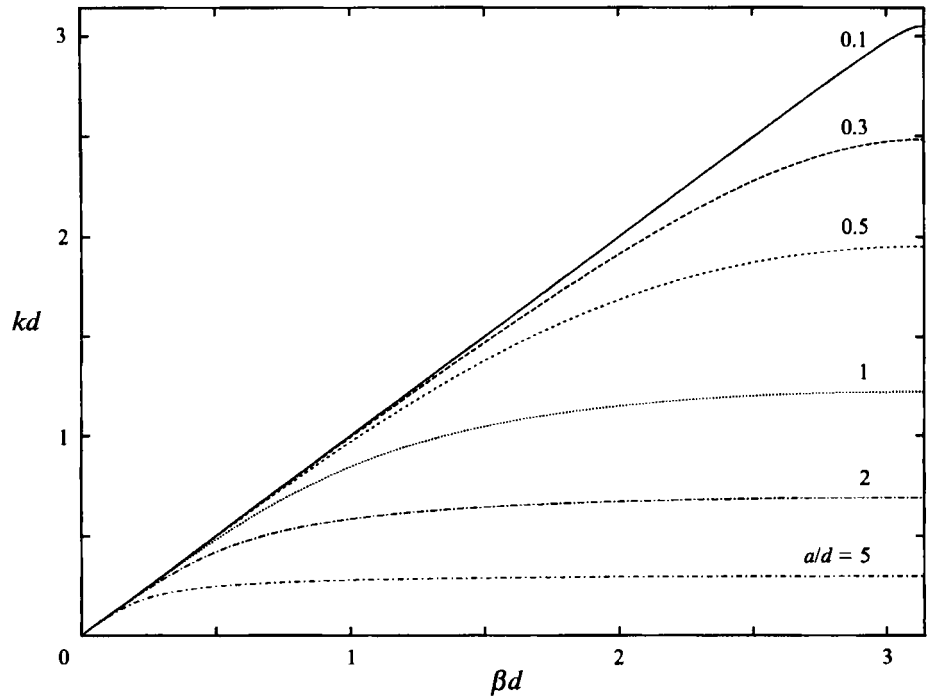

FIGURE 4. Plots of kd against βd for various values of a/d where $b/d = 0.6$.

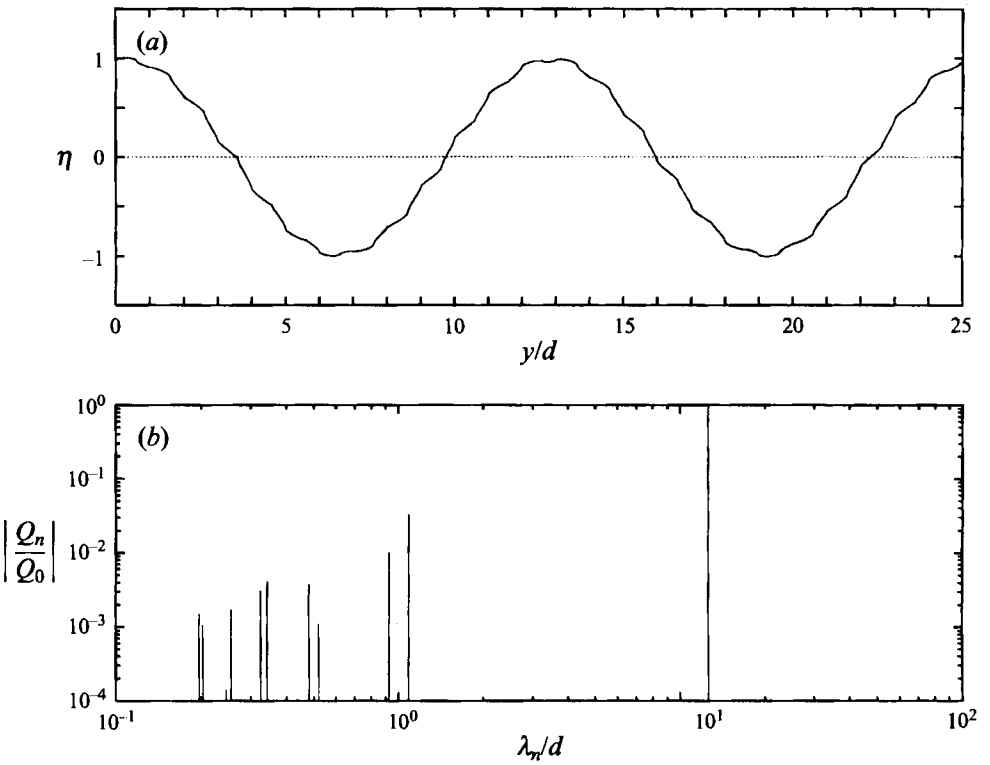

FIGURE 5. (*a*) Surface profile and (*b*) spectral plot for the edge wave $\beta d = 0.5$ with the calculated wavenumber $kd = 0.4809$.

$A \approx \tilde{A}$ we must find the roots of the equation (2.31) which will provide the desired relation between β and k for a given geometry. The parameters of the problem are a/d, b/d relating to the geometry, $\beta d < \pi$, the dimensionless wavenumber of the fundamental edge mode, and $kd (< \beta d)$, related to the frequency $\omega/2\pi$ through (2.2). All four parameters are contained in the two series defining K_{mn} in (2.50). Note that for large r the rth term of each of these series is $O(r^{-7/3})$ and this is sufficient for K_{mn} to be computed to any desired accuracy as a function of all four parameters. In practice $r = 500$ was generally sufficient to give at least three-figure accuracy in the elements K_{mn}. Convergence of $\tilde{A}$ with increasing N proves to be extremely rapid, with $\tilde{A}$ converging to three significant figures for $N \geqslant 4$.

Having evaluated $\tilde{A}$, the approximation to A, it remains to determine numerically the solutions of (2.31). It is not difficult to see that solutions must exist. The dependence of $\tilde{A}$ on a/d occurs through the terms $\coth \alpha_r a$ in K_{mn} as given by (2.64). It is clear that as a/d increases $\tilde{A}$ rapidly approaches a value independent of a/d, given by (2.49) where the a_m are obtained by solving (2.46) with the term $\coth \alpha_r a$ in K_{mn} replaced by unity. Now for fixed kd, $\tan ka$ takes all real values as a/d varies between $(N - 1/2)\pi/kd$ and $(N + 1/2)\pi/kd$, N an integer, and it follows that for fixed b/d, βd, kd there must exist such a value of a/d for which (2.31) is satisfied. Indeed the same argument shows that there is an infinity of values of a/d for each set of values of kd, b/d, βd, the difference between successive values approaching π/kd as a/d increases. This is illustrated by figure 2 which shows how the roots kd of (2.31) vary with a/d for fixed values of $b/d = 0.4$ and various βd. These and

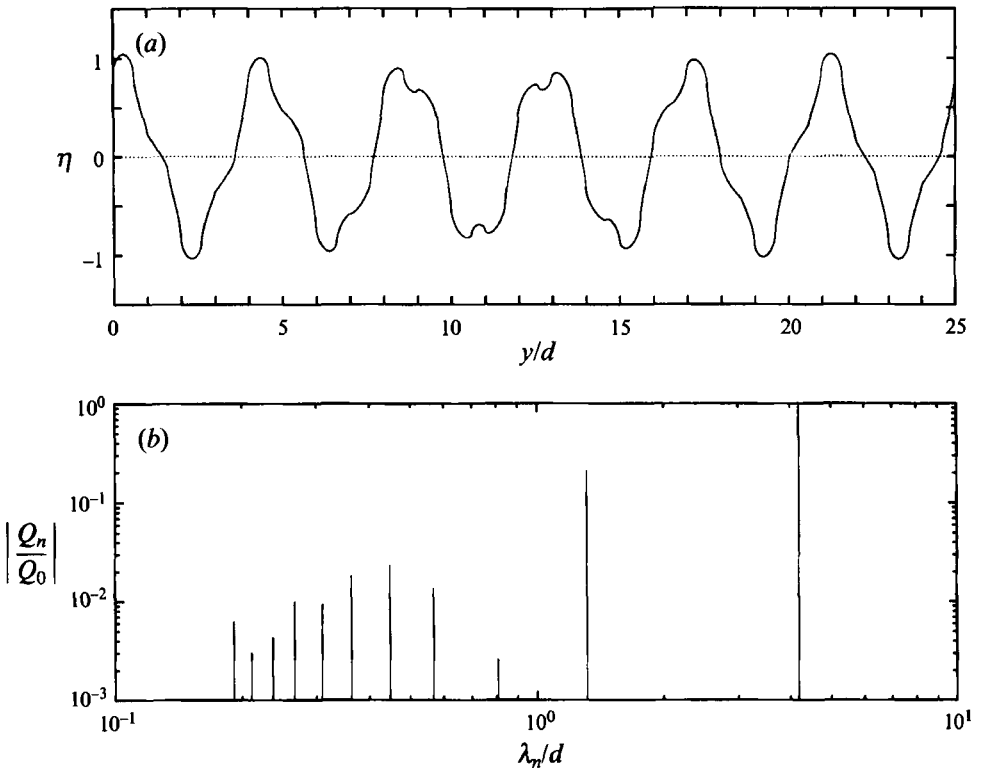

FIGURE 6. (*a*) Surface profile and (*b*) spectral plot for the edge wave $\beta d = 1.5$ with the calculated wavenumber $kd = 1.0457$.

subsequent results were obtained by solving the equation $\tilde{A} - kb\tan ka = 0$. It can be shown that there are at least $M(=[\beta a/\pi]$, [ ] denotes integer part of) roots bounded by $n\pi < ka < (n+1/2)\pi$, $n = 0, 1, \ldots, M-1$, with the possibility of a further root bounded by $M\pi < ka < \tau a$ if $\tilde{A}|_{k=\tau} \leqslant \tau b \tan \tau a$ where $\tau = \min\{(M+1/2)\pi/a, \beta\}$.

Notice how a particular kd decreases monotonically as a/d increases for fixed βd, b/d, with further roots corresponding to higher-frequency edge-wave modes appearing for large values of a/d. Note also how $k \to \beta$ as $a/d \to 0$ for fixed βd, b/d. Figure 2 can be compared to the corresponding figure 2 in Part 1 where $b/d = 1$.

The variation of kd with b/d for a fixed value of $a/d = 0.5$ and various βd is shown in figure 3 where it can be seen that the effect of b/d is small except for the larger values of βd. It appears that for a given βd there is a value of b/d for which the edge wave has a minimum value of kd. This is more discernible for larger values of βd. There are two limiting cases which can be derived from figure 3. First is the case $\beta d = \pi$ corresponding to the standing wave solution (2.73) which is equivalent to the trapped modes described by Evans & Linton (1991) for a rectangular block in a channel. In fact the highest curve in figure 3 corresponding to $\beta d = \pi$ can be compared to the lowest curve in figure 4 of Evans & Linton (1991) where allowance is made for the different definitions of $b/d(= 1-b/d)$ and $d(= 2d)$ in the two papers. The agreement is good and in the present case no problem was encountered in computing the solution as $b/d \to 0$ corresponding to the vanishing of the gaps between successive blocks. It is clear from figure 3 that in this case $k \to \beta$ for all βd. The second limiting case corresponds to the case $b/d = 1$ when the block reduces to a thin barrier, and

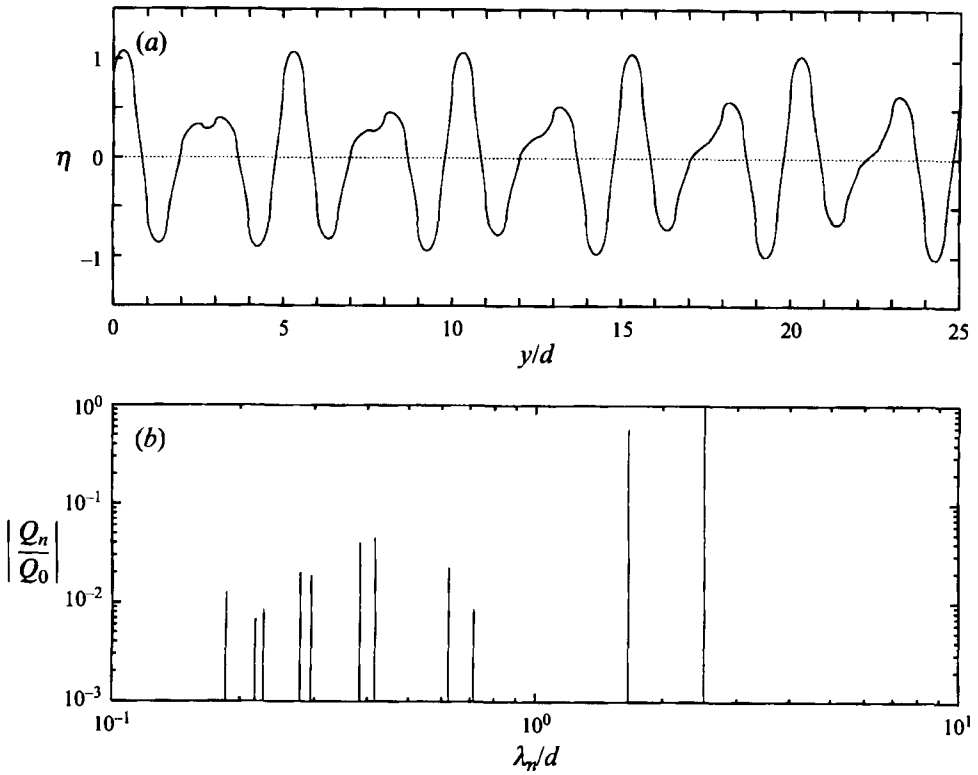

FIGURE 7. (*a*) Surface profile and (*b*) spectral plot for the edge wave $\beta d = 2.5$ with the calculated wavenumber $kd = 1.2008$.

which was considered in Part 1. Thus the end point ($b/d = 1$) of each curve in figure 3 agrees with the corresponding values for k (with $d = 1$) for $a/d = 0.5$ in Part 1.

Figure 4 shows how the fundamental edge-wave frequency, through kd and equation (2.2), varies with βd for fixed $b/d = 0.6$ and various a/d. Only values of $\beta d < \pi$ are presented because the curve is symmetric about π from the argument beginning at (2.36). The values increase monotonically with βd and, regarded as a function of βd, kd appears to have zero gradient at $\beta d = \pi$, and gradient unity at $\beta d = 0$.

Figures 5–9 provide different illustrations of the four-parameter set $\{kd, \beta d, a/d, b/d\}$ which defines an edge wave. For each set of values we can construct the free-surface elevation throughout the flow field by using equations (2.74) to (2.78). Notice from (2.74) that the elevation is not periodic in the y-direction unless $\beta d/2\pi$ is of the form p/q, where p, q are integers with $0 < p < q$. In this case the individual edge-wave modes have wavelengths $\lambda_n = qd/|p + nq|$, $n = 0, \pm 1, \pm 2, \ldots$, the combined edge-wave having period qd in y.

In computing the free-surface elevations we first fix the geometry by choosing typical values of $a/d = 1$, $b/d = 0.6$ and $h/d = 1$. We then choose different βd or the fundamental wavelength of the edge wave which then enables us to determine kd and hence, through (2.2), the corresponding wave frequency or period of the edge waves.

Equation (2.74) is then used, with $x = t = 0$, to plot the free-surface elevation at the blocks, at time $t = 0$, as a function of y/d. For each plot the corresponding values of Q_n and their wavelengths λ_n are plotted showing the relative importance of each mode. For all the spectral plots we have only plotted Q_n against λ_n/d

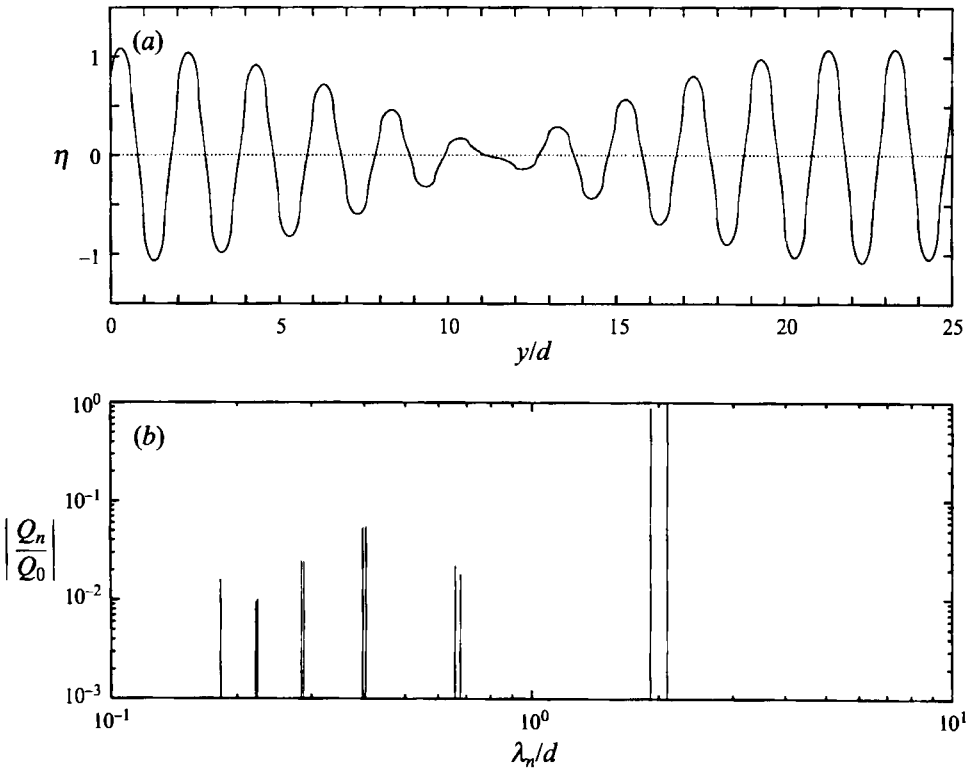

FIGURE 8. (*a*) Surface profile and (*b*) spectral plot for the edge wave $\beta d = 3.0$ with the calculated wavenumber $kd = 1.2209$.

for $n = -5,\ldots,5$ as the higher modes are in general far smaller. Note that each mode is not labelled on the graph but is easily worked out since the λ_n are ordered, $\lambda_0 > \lambda_{-1} > \lambda_1 > \lambda_{-2} > \ldots > \lambda_{-m} > \lambda_m$.

For example figure 5(*a*) shows the surface profile for $\beta d = 0.5$ for which the corresponding wavenumber turns out to be $kd = 0.4809$. The profile is not periodic, and is dominated by the fundamental wavenumber βd which in this case corresponds to a wavelength $4\pi d$. The distortion due to higher modes is slight as is clear from figure 5(*b*) which shows the relative magnitude of Q_n.

The effect of increasing βd to 1.5 is shown in figure 6(*a*) where the corresponding wavenumber is $kd = 1.0457$. The profile is again not periodic with dominant wavelength $4\pi d/3$ but now the effect of the higher modes is evident in the distortion of the profile, and is also confirmed by figure 6(*b*), where now Q_{-1} is 21% of Q_0.

Further plots for values of $\beta d = 2.5$, 3.0 and π in figures 7(*a*,*b*), 8(*a*,*b*) and 9(*a*,*b*) respectively show a transition from a formless aperiodic profile ($\beta d = 2.5$) to a near sinusoidal profile ($\beta d = \pi$). In figure 8(*a*) we see that the surface profile is now modulated by a larger wavelength or 'beat' frequency. The reason for this can be seen in figure 8(*b*) where the different wavelengths are seen to be close together. For $\beta d = \pi$, we know the edge wave reduces to a standing wave and the profile is shown in figure 9(*a*) where it is seen to be periodic with period $2d$ and near sinusoidal. The extent of the higher modes is shown in figure 9(*b*) where the values have merged such that $Q_n = Q_{-n-1}$ and $\lambda_n = \lambda_{-n-1}$. Finally figure 10(*a*,*b*) shows the case of $\beta d = 5\pi/8$ when the profile is periodic with period $16d$.

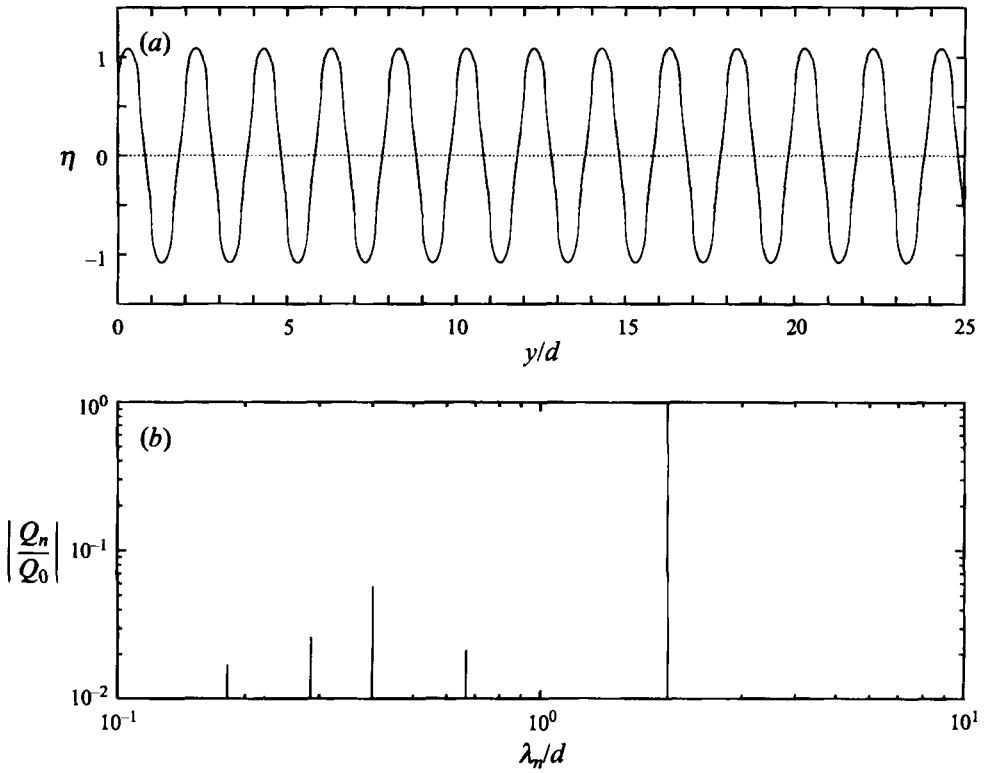

FIGURE 9. (*a*) Surface profile and (*b*) spectral plot for the edge wave $\beta d = \pi$ with the calculated wavenumber $kd = 1.2219$.

In these typical examples only the profiles at $x = 0$ and for $t = 0$ have been shown. As x increases the profiles will change as the amplitudes Q_n are each affected by the term $\exp(-\gamma_n x)$ by different amounts, but the overall profile will reduce rapidly to zero because of this term. For fixed x and each t a different profile is obtained since although the amplitudes Q_n remain the same, the phases will vary with varying t.

4. Conclusion

It has been shown how edge waves which propagate along a cliff face and decay out to sea can occur if there exists a periodic array of rectangular obstacles protruding from the cliff face and extending throughout the water depth. The problem is identical to the construction of Rayleigh–Bloch surface waves along a rectangular diffraction grating in acoustics.

The method of construction is highly efficient numerically, making use of physically relevant expansion functions in a Galerkin approximation to the solution of a certain integral equation. Edge waves appear to occur for all geometries in the sense that for given values of a/d, b/d and wave frequency, through kd, there exists a fundamental mode of wavelength $2\pi/\beta$ which forms the basis, through superposition, of an edge wave solution. Although periodic in time, only in special circumstances is the overall solution periodic in space but since in many cases it appears that the fundamental mode dominates, we shall continue to call them edge waves.

It would appear unlikely that there is anything special about the rectangular

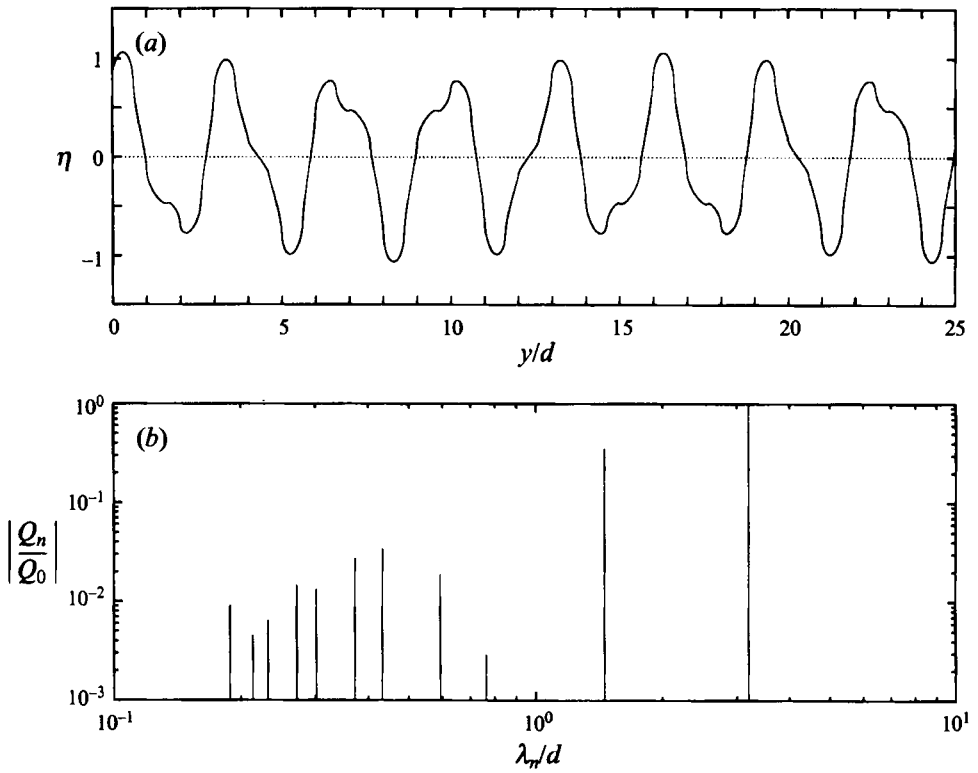

FIGURE 10. (*a*) Surface profile and (*b*) spectral plot for the edge wave $\beta d = 5\pi/8$ with the calculated wavenumber $kd = 1.1434$.

geometry used here and such edge-wave solutions can be expected to occur for more general periodic arrays. For the next simplest case of semicircular cylinders projecting from the cliff face, in personal communications, both L. Mulholland, using a formulation due to Twersky (1962) and C. M. Linton, using a multipole approach, have provided numerical evidence of their existence.

It is possible that the general existence proof provided by by Evans, Levitin & Vassiliev (1994) for trapped modes in the vicinity of a body in a channel could be adapted to the more general periodic array.

We are grateful for one reviewer who has pointed out that an axisymmetric version of the present problem for electromagnetic surface waves along a corrugated infinite wire has been discussed by Jones (1986, pp. 400–402). There is little doubt that the accurate Galerkin expansions used here could be adapted to provide efficient computations of the surface-wave frequencies as a function of the geometry in this case also and work on this problem is in hand.

REFERENCES

ERDÉLYI, A., MAGNUS, W., OBERHETTINGER, F. & TRICOMI, F. G. 1954 *Tables of Integral Transforms.* Bateman manuscript project, vol. 1. McGraw-Hill.

EVANS, D. V. 1992 Trapped acoustic modes. *IMA J. Appl. Maths* **49**, 45–60.

EVANS, D. V., LEVITIN, M. & VASSILIEV, D. 1994 Existence theorems for trapped modes. *J. Fluid Mech.* **261**, 21–31.

EVANS, D. V. & LINTON, C. M. 1991 Trapped modes in open channels. *J. Fluid Mech.* **225**, 153–175.

EVANS, D. V. & LINTON, C. M. 1993 Edge waves along periodic coastlines. *Q. J. Mech. Appl. Maths* **46**, 644–656 (referred to herein as Part 1).

JONES, D. S. 1953 The eigenvalues of $\nabla^2 u + \lambda u = 0$ when the boundary conditions are given semi-infinite domains. *Proc. Camb. Phil. Soc.* **49**, 668–684.

JONES, D. S. 1986 *Acoustic and Electromagnetic Waves.* Science Publications, Oxford.

MITTRA, R. & LEE, S. W. 1971 *Analytical Techniques in the Theory of Guided Waves.* Macmillan.

PETIT, R. 1980 *Electromagnetic Theory of Gratings.* Topics in Current Physics. Springer.

PORTER, R. 1995 PhD thesis, University of Bristol, in preparation.

PORTER, R. & EVANS, D. V. 1995 Complementary approximations to wave scattering by vertical barriers. *J. Fluid Mech.* **294**, 155–180.

STOKES, G. G. 1846 Report on recent researches in hydrodynamics. *Brit. Assoc. Rep.*

TWERSKY, V. 1962 On scattering of waves by the infinite grating of circular cylinders. *IRE Trans. Antennas Propagation* **10**, 737–765.

URSELL, F. 1952 Edge waves over a sloping beach. *Proc. R. Soc. Lond.* A **214**, 79–97.

WILCOX, C. H. 1984 *Scattering Theory for Diffraction Gratings.* Springer.